International Journal of Health Sciences
Available online at www.sciencescholar.us
E-ISSN: 2550-696X
Int. J. of Health Sci.
DOI: 10.53730

How to Cite:
Hassan, S. S., Shebl, M. M., Emam, M. N., Ahmed, A. A., & Madi, M. M. (2025). Reno-protective effect of agmatine in methotrexate-induced kidney injury in rats. *International Journal of Health Sciences*, *9*(S1), 281–297. https://doi.org/10.53730/ijhs.v9nS1.15697

Reno-protective effect of agmatine in methotrexate-induced kidney injury in rats

Samar Shaban Hassan
Assistant Lecturer of Physiology, Faculty of Medicine, Tanta University, Tanta, Egypt
Email: samar.shaban@med.tanta.edu.eg

Mohamed Mohamed Shebl
Assistant Professor of Physiology, Faculty of Medicine, Tanta University, Tanta, Egypt
Email: mmshebl59@yahoo.com

Marwa Nagy Emam
Professor of Physiology, Faculty of Medicine, Tanta University, Tanta, Egypt
Email: maroo_drmaroo@yahoo.com

Abeer Abed Ahmed
Professor of Physiology, Faculty of Medicine, Tanta University, Tanta, Egypt
Email: abeer.abozeid2@yahoo.com

Mohamed Mohamed Madi
Professor of Physiology, Faculty of Medicine, Tanta University, Tanta, Egypt
Email: Dr.mohamedmadi@yahoo.com

***Abstract*---Background:** L-arginine's endogenous metabolite agmatine (AGM) is recognized to have anti-inflammatory, anti-apoptotic, and antioxidant qualities. Investigating the dose-dependent renal-protective effect of AGM in rats with MTX-induced kidney damage was the goal of this study. **Methods:** In this experimental study, fifty male rats were divided into five groups (n = 10). Group I (control) received oral saline for 7 days and IP saline on day 7. Group II (MTX) received oral saline for 7 days and IP MTX (20 mg/kg) on day 7. Groups III–V

***Corresponding author**: Hassan, S.S.; Email: samar.shaban@med.tanta.edu.eg*
Submitted: 27 May 2025, Revised: 18 June 2025, Accepted: 09 July 2025

received AGM orally at 10, 20, and 40 mg/kg/day for 7 days, followed by IP MTX (20 mg/kg) on day 7. **Results:** Intraperitoneal MTX (20 mg/kg) significantly increased renal somatic index, MDA, 8-OHdG, NO, TNF-α, IL-1, serum creatinine, BUN, and NF-κB, while it decreased GSH, SOD, HO-1 activity, Nrf2 expression, and creatinine clearance. AGM administration at various doses showed a protective renal effect against MTX-induced changes. **Conclusions:** Many disorders can be effectively treated with MTX. The toxicity of MTX, which includes nephrotoxicity with a mechanism involving inflammation and oxidative damage, frequently limits its therapeutic uses.

***Keywords*---**Agmatine, Methotreaxate, Oxidative Stress, Rats, Renal Toxicity.

1. Introduction:

The condition known as acute kidney injury (AKI) is characterized by a significant loss of renal function. It also causes chronic kidney disease, has a high death rate, and requires long-term care (Zager, 2015). Psoriasis, rheumatoid arthritis, lupus erythematosus, and neoplastic conditions are all treated with the disease-modifying drug methotrexate (MTX), a dihydrofolate reductase inhibitor (Heidari et al., 2018). While the most frequently reported mechanism of MTX nephrotoxicity is crystallization in the renal tubules, additional mechanisms have also been reported (Kolli, Abraham, Isaac, & Selvakumar, 2009).

Apoptosis signaling pathways, P38 mi-togen-activated protein kinase (P38MAPK)/nuclear factor kappa-light-chain-enhancer of activated B cells (NF-κB), and Kelch-like ECH-associated protein1 (Keap1)/nuclear factor erythroid 2–related factor2 (Nrf2) are some of the molecular pathways that impact kidney pathophysiology (Li et al., 2018). The endogenous metabolite of L-arginine, agmatine (AGM), has anti-inflammatory, anti-apoptotic, and antioxidant qualities (El-Sherbeeny, Nader, Attia, & Ateyya, 2016).

By inhibiting inducible NO synthase (iNOS) and activating endothelial NO synthase (eNOS), AGM influences the synthesis of nitric oxide (NO) (Auguet, Viossat, Marin, & Chabrier, 1995). An earlier study found that NO produced from eNOS suppresses NF-κB activity, which in turn suppresses iNOS expression and the generation of inflammatory cytokines, thereby reducing airway inflammation (Broeke et al., 2006). Investigating the renal-protective effect of AGM in rats with MTX-induced kidney damage was the goal of this study.

2. Subjects and Methods:

2.1. Drugs:

The 50mg/2ml ampoule of MTX was acquired from Algomhoria Pharmaceutical Company. Each animal received a dose of 20 mg/kg, which was determined by its weight. The dose was then diluted in 0.5 ml of sterile normal saline solution

and delivered intraperitoneally as a single dose. Based on previously published research, the ideal MTX dosages and time were established. The high dosage of MTX used in people is directly linked to the dose they used (20 mg/kg) (Howard, McCormick, Pui, Buddington, & Harvey, 2016).

The Sigma Aldrich business supplied the AGM, and the dosage was determined for each animal based on its weight before it was dissolved in saline and administered orally via endogastric tube (Bergin et al., 2019). The stability of AGM in saline for at least four and seven days at room temperature and four degrees Celsius, respectively (Kale et al., 2020).

2.2. Animals

Fifty male rats of the local strain, weighing between 150 and 250 grams, were used in this experimental investigation. Over the course of their employment, the rats were kept in separate animal cages at ambient temperature, subjected to 12-hour cycles of light and dark, and given unrestricted access to tap water and pelleted laboratory feed. The experiment was conducted in compliance with Ethical Issues committee rules (code 35231/1/22).

2.3. Experimental design:

The animals were housed in metabolic cages for a week in order to collect urine, and then for 24 hours after receiving an MTX injection. Under general anesthesia, all of the animals were scarified by cervical dislocation, and blood samples were taken for biochemical examination using intraperitoneal injections of 16 mg xylazine and 60 mg ketamine (Parasuraman, Ching, Leong, & Banik, 2019).

The right kidney was preserved in 10% buffered formalin for NF-kβ immunohistochemistry and histological examinations. Then, in accordance with infection control and safety protocols, each animal was placed in a unique packaging and transported with hospital biohazard.

2.4. Kidney Tissue Homogenate Preparation

To eliminate any red blood cells and clots, the kidney was perfused with a phosphate buffered saline solution with a pH of 7.4 and 0.16 mg/ml heparin before to dissection. Each gram of tissue was homogenized in 5–10 milliliters of cold buffer (50 mM phosphate buffer, pH 7.5). For fifteen minutes, centrifugation was carried out at 4000 r.p.m. After being extracted for analysis, the supernatant was placed in cold storage. If the assay was not performed on the same day, the sample was frozen at -80 °C for at least a month.

2.5. Determination of Serum Creatinine level (Bauer, Brooks, & Burch, 1982):

In an alkaline environment, creatinine in the sample combines with picric acid to create a color complex known as the Jaffè reaction, which absorbs at 492 nm. The amount of creatinine in the sample determines how quickly color forms.

2.6. Determination of Serum urea level (Bauer et al., 1982):
When urea is hydrolyzed with water and urease, ammonia and carbon dioxide are released. In an alkaline pH, free ammonia forms a colored complex in proportion to the specimen's urea concentration when an indicator is present.

2.7. Renal Malondialdehyde (MDA) level (Ohkawa, Ohishi, & Yagi, 1979):
When thiobarbituric acid (TBA) and MDA react in an acidic solution at 95 °C for 30 minutes, the pink product that is produced can be measured at 534 nm for absorbance.

2.8. Determination of 8-Oxo-2-deoxyguanosine (8 Oxo-dG) (Barregard et al., 2013):

Put 8-OHdG into an enzyme well that has already been coated with Rat 8-OHdG monoclonal antibody and incubate it. Next, add 8-OHdG antibodies that have been biotin-labeled and combine with Streptavidin-HRP to create an immunological complex. Finally, repeat the incubation and washing process to get rid of the enzyme that hasn't been coupled. Following the addition of Chromogen Solutions A and B, the liquid's color shifts to blue, and eventually, due to the action of the acid, turns yellow. There was a positive correlation between the color chroma and the concentration of the rat substance 8-OHdG in the sample.

2.9. Washing method

For the procedure, add 50 µl of standard and 50 µl of Streptavidin-HRP to standard wells, and 40 µl of sample, 10 µl of 8-OHdG antibody, and 50 µl of Streptavidin-HRP to test wells. Lightly shake the sealing membranes and incubate at 37°C for 60 minutes. Dilute the 30× washing concentrate with water (30 times) for cleaning, then carefully remove the memento, drain liquid, and shake out excess water. Add 50 µl each of Chromogen solutions A and B to each well, mix gently, and incubate at 37°C for 10 minutes, away from light. To stop the reaction, add 50 µl of Stop Solution, causing the blue color to turn yellow. Finally, measure the optical density (OD) at 450 nm within 15 minutes using the blank well as a reference.

2.10. Renal Reduced Glutathione (GSH) level (Moron, Depierre, & Mannervik, 1979)

By reducing 5,5 dithiobis (2-nitrobenzoic acid) (DTNB) with reduced GSH, a yellow compound is produced. It is possible to quantify the absorbance of the reduced chromogen at 405 nm, which is directly proportional to the amount of GSH.

2.11. Determination of renal superoxide dismutase (SOD) Avidin-HRP Enzymatic Method (Strålin, Karlsson, Johansson, & Marklund, 1995)

Set up wells for the sample, blank, and diluted standards, adding 100 µL of the corresponding solutions to each well. Seal the plate and incubate at 37°C for 2 hours. Remove the liquid without washing, then add 100 µL of the detecting reagent to each well, seal, and incubate at 37°C for 1 hour. Wash the plate with 300 µL of 1× Wash Solution, rinse with tap water, and perform three more

washes, ensuring all liquid is removed. Afterward, add 100 µL of Detection Reagent B, seal, and incubate for 1 hour at 37°C. Add 90 µL of substrate solution to each well, seal, and incubate at 37°C for 15-25 minutes, avoiding exposure to light. Add 50 µL of stop solution, which will turn the liquid yellow. Gently mix by tapping the plate and ensure no bubbles or fingerprints are present. Once the microplate reader is ready, take readings at 450 nm.

2.12. Determination of renal nitric oxide (NO) Azo Dye Colorimetric Method (Montgomery & Dymock, 1961)

N-(1–naphthyl) ethylenediamine is coupled with the nitrous acid that is produced when sulphanilamide is diazotized in an acidic media with nitrite present. At 540 nm, the resultant azo dye, which has a vivid reddish-purple hue, may be quantified.

2.13. Determination of Renal TNF-α level (Wang et al., 2007)

This ELISA kit uses a two antibody sandwich technique to detect rat TNF-α. TNF-α forms a complex with wells that have been pre-coated with monoclonal antibodies, biotin-labeled antibodies, and streptavidin-HRP. Following washing, the addition of acid causes Chromogen Solutions A and B to change color from blue to yellow, signifying the presence of TNF-α.

2.14. Determination of renal interleukin- 1β (IL-1β) Monoclonal Antibody-Based Sandwich ELISA Method (Di Vita et al., 2008)

The MBS Rat IL-1β ELISA kit uses a sandwich approach based on monoclonal antibodies to quantify IL-1β in samples. HRP-streptavidin and biotinylated detection antibody attach to antibody-coated wells after IL-1β. Following washing, the TMB substrate changes color in accordance to the amounts of IL-1β, turning yellow when exposed to stop solution. At 450 nm, absorbance is measured.

2.15. Determination of renal heme oxygenase-1 (HO-1) (Heme Oxygenase-1 EIA (Ozawa et al., 2002)

The sandwich method uses two rat monoclonal anti-HO-1 antibodies to detect rat HO-1 in two phases. One of the rat monoclonal anti-HO-1 antibodies (blocked against non-specific binding) is present in the microtiter plate that holds the incubated samples and standards. Next came the addition of the second anti-HO-1 tagged with peroxidase (POD). Thus, POD-anti-HO-1 tags rat HO-1 on one side and links it to anti-HO-1 (solid phase) on the other. The reaction between POD and substrate (H2O2 and tetramethylbenzidine) results in color development with intensities proportional to the amount of rat HO-1 present in samples and standards. Rat HO-1 levels can be measured by measuring the absorbance using an ELISA Immunoassay (EIA) plate reader. By contrasting the specific absorbance of the samples with that of the standards displayed on a standard curve, the precise quantity of rat HO-1 may be determined.

2.16. Quantitative measurement of nuclear factor gene (nrf2) in kidney tissue: Relative gene expression by quantitative real- time polymerase chain reaction (RT-PCR) (Berger et al., 1999)

To homogenize renal tissue, transfer the cleaned lysate to a microcentrifuge tube and mix with 200 µL of 95% ethanol. Pipette the mixture 3-4 times, then centrifuge in the Spin Column Assembly at 12,000–14,000 rpm for 1 minute. Discard the liquid, refill with the Spin Basket, and add 600 µL of SV wash solution. Centrifuge again for 1 minute. Prepare the DNase mix (5 µL DNase I, 5 µL 0.09M MnCl2, and 40 µL yellow core buffer) and add 50 µL to the Spin Basket. Incubate for 15 minutes, then add 200 µL DNase stop solution and centrifuge. Apply 600 µL SV wash solution with ethanol, then centrifuge for 1 minute. Add 250 µL of ethanol wash solution, centrifuge for 2 minutes. Transfer the Spin Basket to an elution tube, add 100 µL nuclease-free water, and centrifuge for 1 minute. Store RNA at -70°C. Measure RNA yield using a dual spectrophotometer at 260-280 nm. For cDNA synthesis, use 0.5-2 µg RNA with the cDNA reverse transcription kit.

2.17. Histological Examination of Kidney

Examining Kidney Sections Histologically After being dehydrated and embedded in paraffin wax, kidney specimens preserved in 10% buffered formalin were cut into 5-µm slices. The sections were prepared for hematoxylin and eosin (H&E) staining after deparaffinization and rehydration, and they were subsequently inspected.

2.18. Immunohistochemical examination of nuclear factor kappa-B (NF-kB) in kidney (Yamanaka et al., 2004)

For immunohistochemistry examination, the kidney was embedded in paraffin wax after being dehydrated in a series of graded ethanol. Paraffin blocks were cut into sections that were about 2-3 µm thick. These sections were then placed on positively charged lams and incubated for 15 minutes at 70°C. Following deparaffinization in graded xyilol, each portion was hydrated in several absolute (99.8%) alcohol solutions before being washed with distilled water Following the antigen retrieval process, the sections were washed in distilled water and treated with 3% H2O2 using a 0.01 M citrate buffer. Phosphate-buffered saline (PBS/pH = 7.4) was used to rinse the sections. Sections were incubated with the corresponding primary monoclonal antibody, anti-p65 dilution (1:150), for an entire night at 4°C. They used the streptavidin-biotin complex (strept-ABC) method for immunohistochemical staining. Hematoxylin was then used as a counterstain for each region.

2.19. Determination of NF-kB positivity:

NF-kB's positive expression was evaluated using the image J analysis tool.It was presented as an area percentage (Keates, Hitti, Upton, & Kelly, 1997).

2.20. Statistical analysis

For statistical analysis, SPSS v26 (IBM Inc., Chicago, IL, USA) was utilized. The three groups' quantitative variables, represented as mean and standard deviation (SD), were compared using the ANOVA (F) test with post hoc test (Tukey). Presented as frequency and percentage (%), the qualitative variables were

analyzed using the Chi-square test. For statistical significance, a two-tailed P value < 0.05 was used.

3. Results:

Serum creatinine, BUN, RSI, MDA, and 8-Oxo-dG showed a significant decrease in group V compared to group IV (P<0.05). Creatinine clearance, GSH and SOD showed a significant increase in group V compared to group IV (P<0.05). **Table 1** NO, TNF -alpha and IL-1B showed a significant decrease in group V compared to group IV (P<0.05). HO -1 and NRF2 showed a significant increase in group V compared to group IV (P<0.05). **Table 2**

3.1. Renal histopathology

3.1.1. Control group

All animals in this group showed normal kidney tissue regarding the morphology in glomerular and tubular areas with clear brush border of proximal tubules. **(Figure 1, A)**

3.1.2. MTX group

Animals in this group had renal sections stained with H&E, which revealed several abnormalities, including vacuolar degeneration, tubular atrophy, and necrosis. Bowman's space in glomeruli narrows. In certain areas of this group, mild glomerular fibrosis and loss of brush boundary in the proximal tubular epithelium were also noted. congestion and noticeable vascular space dilatation. **(Figure 1, B and C)**

3.1.3. MTX+AGM 10mg group

Animals in this group had kidney sections with reduced renal tissue histological deterioration. The injection of 10 mg of AGM decreased the damage parameters of vascular congestion and Bowman's space narrowing when this group was compared to the Mtx-treated group. Additionally, there was less degradation in the brush border of the proximal tubules and other tubules, however this was less severe than with other dosages. **(Figure 1, D)**

3.1.4. MTX+AGM 20mg group

Animals in this group had kidney sections with reduced renal tissue histological deterioration. The administration of AGM 20mg decreased the damage parameters of vascular congestion and Bowman's space narrowing when this group was compared to the Mtx-treated group. Additionally, the brush border of the proximal tubules and other tubules showed less degradation; yet, this is still more protective than the prior one. **(Figure 1, E)**

3.1.5. MTX+AGM group 40mg

Animals in this group had kidney sections with reduced renal tissue histological deterioration. The administration of AGM 40mg decreased the damage parameters of vascular congestion and Bowman's space narrowing when this group was compared to the Mtx-treated group. showed reduced degradation in the proximal tubules' and other tubules' brush borders, but this dosage Out of the three doses, this one is the most protected. **(Figure 1, F)**

3.1.6. Imunohistochemical analysis of NF-KB of all groups: were presented in **Figure 2**

4. Discussion

ARF, sometimes referred to as AKI, is a rapid deterioration in kidney function. ARF can appear in a matter of hours to days, and in order to avoid serious consequences and enhance patient outcomes, it frequently necessitates immediate medical attention (Tomsa, Alexa, Junie, Rachisan, & Ciumarnean, 2019).

In the current study, IP injection of MTX at a dose of 20 mg/kg resulted in a significant decrease in creatinine clearance, GSH, SOD, HO-1 activity, and Nr F2 expression and a significant increase in serum creatinine level, BUN level, RSI, MDA, 8-Oxo-dG, NO content, TNF alpha, and IL-1B. In contrast, administration of AGM at varying doses demonstrated a protective renal effect against the effects of MTX.

The current study assessed the role of AGM in preventing AKI caused by oxidizing agents such as MTX. The anti-inflammatory effect of AGM may be the cause of this effect. Han et al. (Han, Yu, Song, Luo, & Wu, 2015) reported that AGM shields Müller cells from high concentration glucose-induced cell damage.

By dramatically raising SOD activity in the renal tissue, AGM in our investigation counteracted the effects of MTX. AGM's capacity to counteract the rise in free radicals brought on by MTX may be the origin of the apparent ameliorative effect. According to this study, administering MTX raised the amount of NO in renal tissue; however, AGM totally undid this effect. AGM suppresses NO production by lowering iNOS activity and protein levels in macrophages and astrocytes. These findings support the molecular basis of AGM's anti-inflammatory impact and are consistent with those of Łuczak et al. (Łuczak, Madej, Kasprzyk, & Doroszko, 2020).

According to Miranda-Mosqueda et al. (Miranda-Mosqueda, Ruiz-Oropeza, & Gomez-Acevedo, 2024). AGM also influences the permeability of the mitochondrial membrane by preventing the Ca 2+-dependent activation of the mitochondrial permeability transition in the rat brain.

By activating NF-κB, the released NO may combine with superoxide anions to create peroxynitrite and promote the generation of pro-inflammatory cytokines. NF-κB controls the transcriptional expression of pro-inflammatory cytokines and iNOS.

AGM was able to lower TNF-α and IL-1β levels as well as NF-κB expression in the current study. One possible explanation for this anti-inflammatory impact is the inhibition of NF-κB production. Furthermore, RNS may be avoided by inhibiting iNOS. formation of reactive nitrogen species, which inhibits the release of inflammatory cytokines. These results were consistent with those of Li et al. (Li et al., 2018).

In the kidney of rats given MTX, increased and prolonged ROS production can suppress nuclear factor erythroid 2–related factor 2 (Nrf2) signaling. The main function of Nrf2, which is strictly regulated, is to combat oxidative stress. Downregulation of the Nrf2 pathway is a direct result of long-term MTX-induced ROS. Together with HO-1, nuclear localized Nrf2 in oxidative stress status increases antioxidation activity and activates anti-inflammatory cytokines. In addition to directly inhibiting proinflammatory cytokines and NF-κB signaling, the absence of Nrf2 triggered inflammation by activating proinflammatory mediators and NF-κB (Abd El-Twab, Hussein, Hozayen, Bin-Jumah, & Mahmoud, 2019).

Numerous downstream cytoprotective proteins and enzymes, including HO-1, which has a renoprotective impact against AKI, are regulated by Nrf2, a key transcriptional regulator against oxidative stress (Nezu & Suzuki, 2020).

Renal Nrf2 and HO-1 were both increased at the protein level by AGM therapy in a dose-dependent manner. AGM's antioxidant effect on HO-1 was previously reported to be attributed to its regulation of the Nrf2 pathway, which was mediated by α2-adrenergic and 5-HT2A receptors as well as the PI3K/Akt signaling pathway.This result was in agreement with Sharawy et al. (Sharawy, Abdelrahman, & El-Kashef, 2018) who reported that AGM attenuates rhabdomyolysis-induced AKI in rats in a dose-dependent manner.

Urea and creatinine, two indicators of renal function, are frequently utilized as measures of glomerular function and are crucial in the diagnosis of renal injury and evaluation of kidney function. Deterioration of renal function is indicated by an increase in these blood indicators According to the current study's findings, the MTX-treated group's urea and creatinine levels significantly increased, as was previously documented (Aladaileh et al., 2019).

Ultrastructural changes further validated the kidney damage caused by MTX. Serum urea and creatinine levels were shown to increase in conjunction with renal impairment and delayed MTX elimination (Howard et al., 2016).

According to the study's findings, giving MTX to Wistar rats resulted in a typical pattern of nephrotoxicity, which was shown by a noticeable rise in blood urea nitrogen and serum creatinine levels. Serum creatinine levels significantly decreased with AGM treatment.

The present investigation demonstrated that the increasing decrease in creatinine clearance following MTX treatment resulted in a decrease in GFR. This outcome was in agreement with Sah et al. (Sah, Subramanian, & Ramesh, 2020) The administration of AGM resulted in a notable rise in creatinine clearance. This outcome was consistent with Ommati et al. (Ommati et al., 2020).

For Low Doses of AGM, 10 mg offered some protection against MTX-induced kidney damage by moderately lowering inflammation and oxidative stress, which led to a minor improvement in renal function indicators such as serum creatinine and BUN levels. This was further supported by kidney histology, which revealed a slight decrease in tubular damage, interstitial inflammation, and apoptotic cell death in rats given low doses of AGM as opposed to controls given MTX.

Nevertheless, the protection was not total, and focal necrosis of glomerular epithelial cells, clogged blood vessels, and the infiltration of mononuclear inflammatory cells are still signs of some renal damage. This is in line with what Salihoglu et al. (Salihoglu et al., 2016) evaluated the protective effect of AGM against cisplatin nephrotoxicity with 99mTc-DMSA renal scintigraphy and cystatin-C using a dose 10 mg AGM.

Renal dysfunction is indicated by elevated levels of certain kidney damage biomarkers. The histological changes further supported the AKI caused by MTX. Leukocyte infiltration, degenerative glomerular and tubular epithelial cell alterations, interstitial bleeding, and other conditions were observed in kidney sections. Prior research that linked MTX treatment to changed renal function and histological features corroborated these findings (Elseady, Keshk, Elhanafy, & Abd Ellatif, 2023). Tubular blockage and impaired renal clearance are the results of MTX and its 7-hydroxy metabolite precipitating in the renal tubules, which causes kidney damage. In rats inebriated with MTX, AGM remarkably provided protection and improved kidney function, suggesting a strong renoprotective effect. AGM successfully decreased urea and creatinine and stopped the histological changes brought on by MTX. Less renal tissue deterioration was found when kidney sections were examined (Gai, Gui, Kullak-Ublick, Li, & Visentin, 2020).

One of the study's limitations was the very small sample size. Therefore, we advise that more clinical research be done to verify its efficacy and safety in people.

Conclusions

MTX poses a number of risks to renal tissue. Oxidative stress is the result. AGM is a crucial molecule that protects the kidneys. It has the ability to scavenge free radicals and act as an antioxidant. In patients receiving treatment with nephrotoxic medications like MTX or cisplatin, AGM may be utilized as an adjuvant therapy to avoid nephrotoxicity because it also significantly improved all parameters in MTX-induced kidney toxicity.

Acknowledgments:
Nil.

5. References

Abd El-Twab, S. M., Hussein, O. E., Hozayen, W. G., Bin-Jumah, M., & Mahmoud, A. M. (2019). Chicoric acid prevents methotrexate-induced kidney injury by suppressing NF-κB/NLRP3 inflammasome activation and up-regulating Nrf2/ARE/HO-1 signaling. *Inflamm Res, 68*(6), 511-523. doi:10.1007/s00011-019-01241-z

Aladaileh, S. H., Hussein, O. E., Abukhalil, M. H., Saghir, S. A. M., Bin-Jumah, M., Alfwuaires, M. A., . . . Mahmoud, A. M. (2019). Formononetin upregulates Nrf2/HO-1 signaling and prevents oxidative stress, inflammation, and kidney injury in methotrexate-induced rats. *Antioxidants (Basel), 80*(10), 17-25. doi:10.3390/antiox8100430

Auguet, M., Viossat, I., Marin, J. G., & Chabrier, P. E. (1995). Selective inhibition of inducible nitric oxide synthase by agmatine. *Jpn J Pharmacol, 69*(3), 285-287. doi:10.1254/jjp.69.285

Barregard, L., Møller, P., Henriksen, T., Mistry, V., Koppen, G., Rossner, P., Jr., . . . Cooke, M. S. (2013). Human and methodological sources of variability in the measurement of urinary 8-oxo-7,8-dihydro-2'-deoxyguanosine. *Antioxid Redox Signal, 18*(18), 2377-2391. doi:10.1089/ars.2012.4714

Bauer, J. H., Brooks, C. S., & Burch, R. N. (1982). Renal function studies in man with advanced renal insufficiency. *Am J Kidney Dis, 2*(1), 30-35. doi:10.1016/s0272-6386(82)80040-1

Berger, J., Leibowitz, M. D., Doebber, T. W., Elbrecht, A., Zhang, B., Zhou, G., . . . Moller, D. E. (1999). Novel peroxisome proliferator-activated receptor (PPAR) gamma and PPARdelta ligands produce distinct biological effects. *J Biol Chem, 274*(10), 6718-6725. doi:10.1074/jbc.274.10.6718

Bergin, D. H., Jing, Y., Williams, G., Mockett, B. G., Zhang, H., Abraham, W. C., & Liu, P. (2019). Safety and neurochemical profiles of acute and sub-chronic oral treatment with agmatine sulfate. *Sci Rep, 9*(1), 126-150. doi:10.1038/s41598-019-49078-0

Broeke, R. T., De Crom, R., Van Haperen, R., Verweij, V., Leusink-Muis, T., Van Ark, I., . . . Folkerts, G. (2006). Overexpression of endothelial nitric oxide synthase suppresses features of allergic asthma in mice. *Respir Res, 7*(2), 1-13.

Di Vita, G., Patti, R., Sparacello, M., Balistreri, C. R., Candore, G., & Caruso, C. (2008). Impact of different texture of polypropylene mesh on the inflammatory response. *Int J Immunopathol Pharmacol, 21*(1), 207-214. doi:10.1177/039463200802100123

El-Sherbeeny, N. A., Nader, M. A., Attia, G. M., & Ateyya, H. (2016). Agmatine protects rat liver from nicotine-induced hepatic damage via antioxidative, antiapoptotic, and antifibrotic pathways. *Naunyn Schmiedebergs Arch Pharmacol, 389*(12), 1341-1351. doi:10.1007/s00210-016-1284-9

Elseady, W. S., Keshk, W. A., Elhanafy, H. A., & Abd Ellatif, R. (2023). Ameliorative potential of lactoferrin on methotrexate-induced nephrotoxicity in rat: a histological and immunohistochemical study. *Egypt J Histol, 46*(1), 49-64.

Gai, Z., Gui, T., Kullak-Ublick, G. A., Li, Y., & Visentin, M. (2020). The role of mitochondria in drug-induced kidney injury. *Front Physiol, 11*(5), 10-79. doi:10.3389/fphys.2020.01079

Han, N., Yu, L., Song, Z., Luo, L., & Wu, Y. (2015). Agmatine protects Müller cells from high-concentration glucose-induced cell damage via N-methyl-D-aspartic acid receptor inhibition. *Mol Med Rep, 12*(1), 1098-1106. doi:10.3892/mmr.2015.3540

Heidari, R., Ahmadi, A., Mohammadi, H., Ommati, M. M., Azarpira, N., & Niknahad, H. (2018). Mitochondrial dysfunction and oxidative stress are involved in the mechanism of methotrexate-induced renal injury and electrolytes imbalance. *Biomed Pharmacother, 107*(12), 834-840. doi:10.1016/j.biopha.2018.08.050

Howard, S. C., McCormick, J., Pui, C. H., Buddington, R. K., & Harvey, R. D. (2016). Preventing and managing toxicities of high-dose methotrexate. *Oncologist, 21*(12), 1471-1482. doi:10.1634/theoncologist.2015-0164

Kale, M., Nimje, N., Aglawe, M. M., Umekar, M., Taksande, B., & Kotagale, N. (2020). Agmatine modulates anxiety and depression-like behaviour in diabetic

insulin-resistant rats. *Brain Res, 1747*(145), 147-160. doi:10.1016/j.brainres.2020.147045

Keates, S., Hitti, Y. S., Upton, M., & Kelly, C. P. (1997). Helicobacter pylori infection activates NF-kappa B in gastric epithelial cells. *Gastroenterol, 113*(4), 1099-1109. doi:10.1053/gast.1997.v113.pm9322504

Kolli, V. K., Abraham, P., Isaac, B., & Selvakumar, D. (2009). Neutrophil infiltration and oxidative stress may play a critical role in methotrexate-induced renal damage. *Chemotherapy, 55*(2), 83-90. doi:10.1159/000192391

Li, B., Jiang, T., Liu, H., Miao, Z., Fang, D., Zheng, L., & Zhao, J. (2018). Andrographolide protects chondrocytes from oxidative stress injury by activation of the Keap1-Nrf2-Are signaling pathway. *J Cell Physiol, 234*(1), 561-571. doi:10.1002/jcp.26769

Łuczak, A., Madej, M., Kasprzyk, A., & Doroszko, A. (2020). Role of the eNOS Uncoupling and the Nitric Oxide Metabolic Pathway in the Pathogenesis of Autoimmune Rheumatic Diseases. *Oxid Med Cell Longev, 2020*, 1417981. doi:10.1155/2020/1417981

Miranda-Mosqueda, L., Ruiz-Oropeza, S., & Gomez-Acevedo, C. (2024). Neuroprotective effect of agmatine in ischemic vascular events. *Med Res Arch, 12*(1), 17-25.

Montgomery, H., & Dymock, J. (1961). Determination of nitrite in water. Royal soc chemistry thomas graham house, science park, milton rd, cambridge Cb4 0wf. *J Med Lab Technol, 22*(5), 111-118.

Moron, M. S., Depierre, J. W., & Mannervik, B. (1979). Levels of glutathione, glutathione reductase and glutathione S-transferase activities in rat lung and liver. *Biochim Biophys Acta, 582*(1), 67-78. doi:10.1016/0304-4165(79)90289-7

Nezu, M., & Suzuki, N. (2020). Roles of Nrf2 in protecting the kidney from oxidative damage. *Int J Mol Sci, 21*(8), 178-210. doi:10.3390/ijms21082951

Ohkawa, H., Ohishi, N., & Yagi, K. (1979). Assay for lipid peroxides in animal tissues by thiobarbituric acid reaction. *Anal Biochem, 95*(2), 351-358. doi:10.1016/0003-2697(79)90738-3

Ommati, M. M., Farshad, O., Mousavi, K., Taghavi, R., Farajvajari, S., Azarpira, N., . . . Heidari, R. (2020). Agmatine alleviates hepatic and renal injury in a rat model of obstructive jaundice. *PharmaNutrition, 13*(4), 100-121.

Ozawa, N., Goda, N., Makino, N., Yamaguchi, T., Yoshimura, Y., & Suematsu, M. (2002). Leydig cell-derived heme oxygenase-1 regulates apoptosis of premeiotic germ cells in response to stress. *J Clin Invest, 109*(4), 457-467. doi:10.1172/jci13190

Parasuraman, S., Ching, T. H., Leong, C. H., & Banik, U. (2019). Antidiabetic and antihyperlipidemic effects of a methanolic extract of Mimosa pudica (Fabaceae) in diabetic rats. *Egypt. J Basic Appl Sci, 6*(1), 137-148.

Sah, S. K., Subramanian, R., & Ramesh, M. (2020). Methotrexate-induced organ toxicity in patients with rheumatoid arthritis: A review article. *Drug Discov Today, 14*(1), 178-190.

Salihoglu, Y. S., Elri, T., Gulle, K., Can, M., Aras, M., Ozacmak, H. S., & Cabuk, M. (2016). Evaluation of the protective effect of agmatine against cisplatin nephrotoxicity with 99mTc-DMSA renal scintigraphy and cystatin-C. *Ren Fail, 38*(9), 1496-1502. doi:10.1080/0886022x.2016.1227919

Sharawy, M. H., Abdelrahman, R. S., & El-Kashef, D. H. (2018). Agmatine attenuates rhabdomyolysis-induced acute kidney injury in rats in a dose dependent manner. *Life Sci, 208*, 79-86. doi:10.1016/j.lfs.2018.07.019

Strålin, P., Karlsson, K., Johansson, B. O., & Marklund, S. L. (1995). The interstitium of the human arterial wall contains very large amounts of extracellular superoxide dismutase. *Arterioscler Thromb Vasc Biol, 15*(11), 2032-2036. doi:10.1161/01.atv.15.11.2032

Tomsa, A. M., Alexa, A. L., Junie, M. L., Rachisan, A. L., & Ciumarnean, L. (2019). Oxidative stress as a potential target in acute kidney injury. *PeerJ, 7*(4), 80-90. doi:10.7717/peerj.8046

Wang, J., Zhou, G., Chen, C., Yu, H., Wang, T., Ma, Y., . . . Chai, Z. (2007). Acute toxicity and biodistribution of different sized titanium dioxide particles in mice after oral administration. *Toxicol Lett, 168*(2), 176-185. doi:10.1016/j.toxlet.2006.12.001

Yamanaka, N., Sasaki, N., Tasaki, A., Nakashima, H., Kubo, M., Morisaki, T., . . . Katano, M. (2004). Nuclear factor-kappaB p65 is a prognostic indicator in gastric carcinoma. *Anticancer Res, 24*(2), 1071-1075.

Zager, R. A. (2015). Marked protection against acute renal and hepatic injury after nitrited myoglobin + tin protoporphyrin administration. *Transl Res, 166*(5), 485-501. doi:10.1016/j.trsl.2015.06.004

Table 1: The serum creatinine, creatinine clearance, BUN, RSI, MDA, 8-Oxo-dG, GSH and SOD in all studied groups

	G I (control)	G II (MTX)	G III (MTX+AGM 10mg)	G IV (MTX+AGM 20mg)	G V (MTX+AGM 40mg)	F	P
Serum creatinine (mg/dl)	0.973±0.037	3.54±0.24	2.7±0.14	2.56±0.18	1.54±0.26	283.23	<0.05
	P1<0.001*, P2<0.001*, P3<0.001*, P4<0.001*						
Creatinine clearance (ml/min)	34.46±2.197	14.89±1.079	20.5±2.02	28.1±2.117	33.74±3.082	150.12	<0.05
	P1<0.001*, P2<0.001*, P3<0.001*, P4<0.001*						
BUN (mg/dl)	35.89±1.643	120.79±3.272	93.14±1.588	76.6±3.423	49.41±3.239	1511.9	<0.05
	P1<0.001*, P2<0.001*, P3<0.001*, P4<0.001*						
RSI	0.29±0.014	0.47±0.016	0.43±0.008	0.38±0.009	0.34±0.009	358.33	<0.05
	P1<0.001*, P2<0.001*, P3<0.001*, P4<0.001*						
MDA (nmol/g)	4.69±0.34	12.06±0.41	9.47±0.41	7.98±0.38	6.39±0.44	502.71	<0.05
	P1<0.001*, P2<0.001*, P3<0.001*, P4<0.001*						
8-Oxo-dG (ng/100mg)	95.1±3.63	213.3±3.6	155.92±3.78	135.3±2.1	122.24±2.4	1943.9	<0.05
	P1<0.001*, P2<0.001*, P3<0.001*, P4<0.001*						
GSH (µmol/g)	0.0587±0.007	0.0194±0.0015	0.03±0.004	0.04±0.002	0.049±0.002	142	<0.05
	P1<0.001*, P2<0.001*, P3<0.001*, P4<0.001*						
SOD (U/g)	48.36±1.776	39.03±1.715	43.77±1.17	46.89±1.08	49.65±0.59	100.4	<0.05
	P1<0.001*, P2<0.001*, P3<0.001*, P4<0.001*						

Data are presented as mean ± SD. * Significant P value <0.05, P1: comparison with GI, P2: comparison with GII, P3: comparison with GIII, P4: comparison with GIV, MTX: Methotrexate, AGM: Agmatine, BUN: blood urea nitrogen, RSI: renal somatic index, MDA: malondialhyde, 8-Oxo-dG: 8-Oxo-2-deoxygenase, GSH: glutathione, SOD: superoxide dismutase.

Table 2: The NO, TNF -alpha, IL-1B, HO -1 and NRF2 in all studied groups

	G I (control)	G II (MTX)	G III (MTX+AGM 10mg)	G IV (MTX+AGM 20mg)	G V (MTX+AGM 40mg)	F	P
NO (µmol/g tissue)	5.22±0.51	69.13±5.2	20.1±0.89	15.55±0.84	13.72±0.65	1101.7	<0.05
	P1<0.001*, P2<0.001*, P3<0.001*, P4<0.001*						
TNF -alpha (pg/ml)	42.63±3.67	104.6±6.67	72.19±2.11	64.36±2.48	56.05±2.25	366.78	<0.05
	P1<0.001*, P2<0.001*, P3<0.001*, P4<0.001*						
IL-1B (pg/ml)	4.48±0.5	21.67±0.71	11.64±0.57	8.98±0.66	7.1±0.37	1327.1	<0.05
	P1<0.001*, P2<0.001*, P3<0.001*, P4<0.001*						
HO -1 (pg/ml)	22.13±0.25	9.07±0.11	11.02±0.099	14.39±0.83	18.97±1.097	743.8	<0.05
	P1<0.001*, P2<0.001*, P3<0.001*, P4<0.001*						
NRF2 (pg/ml)	11.13±0.15	3.2±0.29	6.61±0.24	7.56±0.38	8.52±0.29	1006.6	<0.05
	P1<0.001*, P2<0.001*, P3<0.001*, P4<0.001*						

Data are presented as mean ± SD. * Significant P value <0.05, P1: comparison with GI, P2: comparison with GII, P3: comparison with GIII, P4: comparison with GIV, MTX: Methotrexate, AGM: Agmatine, NO: nitric oxide,
TNF -alpha: tumor necrosis factor alpha, IL-1B: Interleukin 1, HO -1: heam oxygenase-1, NRF2: nuclear factor erythroid 2 related factor.

Figure Legend:

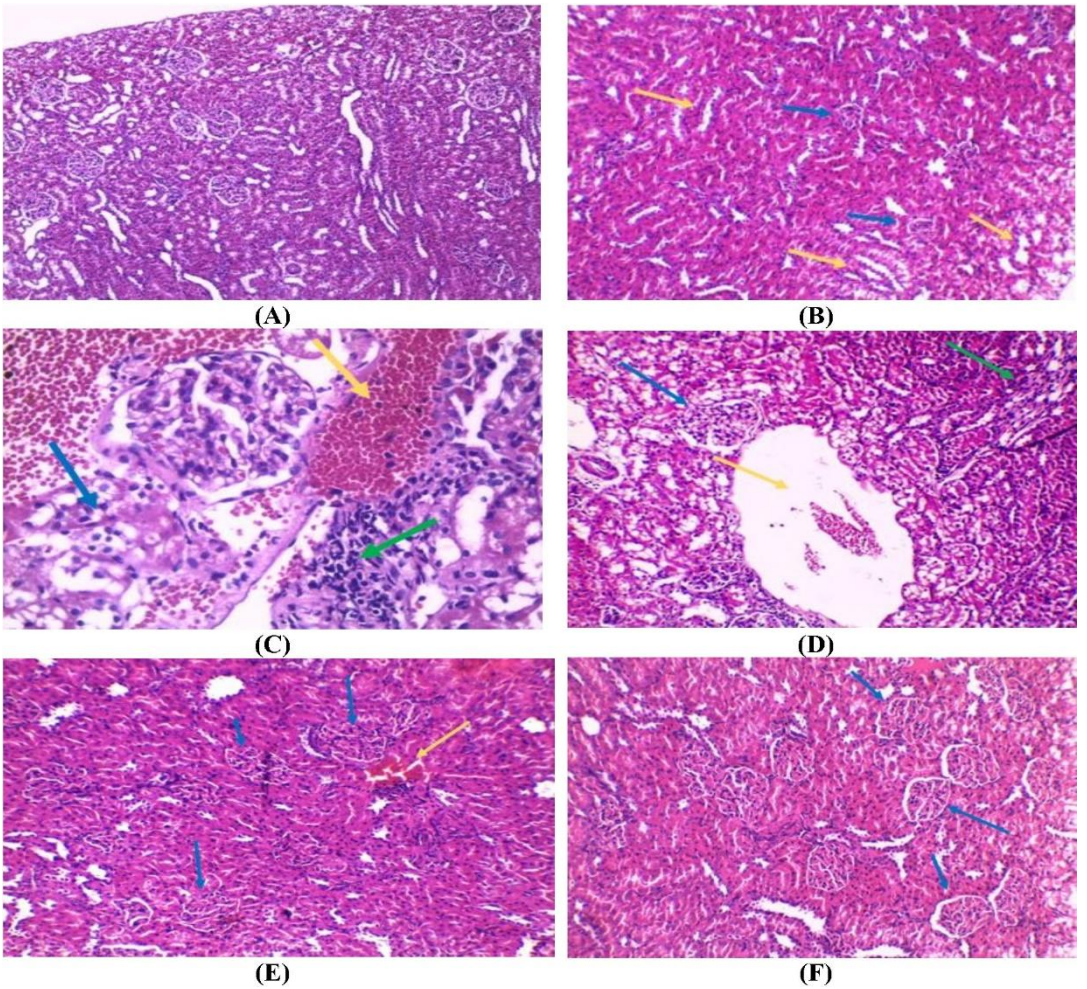

Figure 1: Section from (A) control group showing normal renal glomeruli and tubules. (H&E x100), (B) MTX-intoxicated group showing atrophic necrotic glomeruli (blue arrows) and dilated renal tubules (yellow arrows). (H&E x100), (C) sever renal injury in the form of necrosis in epithelial lining of renal glomeruli (blue arrow) associated with interstitial hemorrhage (yellow arrow) and infiltration by mononuclear inflammatory cells (green arrow). (H&E x400), (D) MTX-intoxicated group pretreated with agmatine (10mg) showed mild protection from renal injury by MTX in the form of focal necrosis of glomerular epithelial cells (blue arrow). Congested blood vessels (yellow arrow) and mononuclear inflammatory cells infiltrate (green arrow) are still seen. (H&E x200), (E) MTX-intoxicated group pretreated with agmatine (20mg) showed moderate protection from MTX effect. Renal glomeruli are uniformly arranged (blue arrows) but blood vessels are still mildly congested (yellow arrow). (H&E x200), (F) MTX-intoxicated group pretreated with agmatine (40mg) showed high protection from renal injury by MTX in the form of uniformly arranged glomeruli without epithelial cells necrosis (blue arrow). No hemorrhage, congested blood vessels or inflammatory cellular infiltrate (H&E x200)

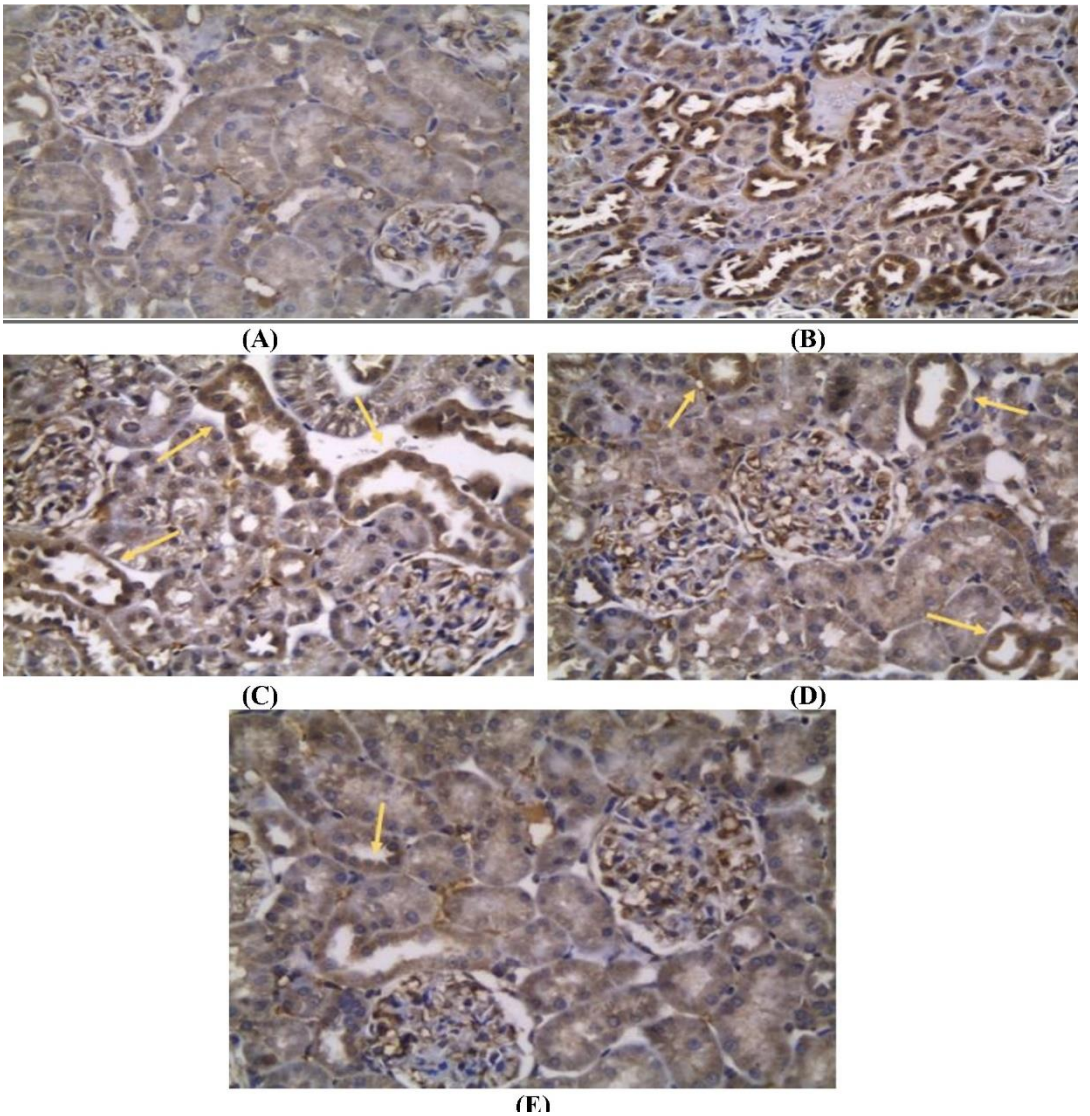

Figure 2: Section from normal (A) control group showed negative expression of NF-KB (IHC x400), (B) MTX-intoxicated group showed high cytoplasmic expression of NF-KB in the epithelial lining of majority of renal tubules indicating toxicity and necrosis by MTX. (IHC x400), (C) MTX-intoxicated group pretreated with agmatine (10mg) showed high cytoplasmic expression of NF-KB in the epithelial lining of some renal tubules (yellow arrows) due to mild protection by agmatine decreasing the necrotic effect of MTX. (IHC x400), (D) MTX-intoxicated group pretreated with agmatine (20mg) showed moderate focal cytoplasmic expression of NF-KB in the epithelial lining of few renal tubules (yellow arrows) due to moderate protective effect of agmatine. (IHC x400), (E) MTX-intoxicated group pretreated with agmatine (40mg) showed weak cytoplasmic expression of NF-KB in focal cells of epithelial lining of renal tubules (yellow arrow) denoting absence of necrosis due to the good protective effect of agmatine. (IHC x400)